Electronic, Magnetic and Fermi Surface properties of Cu_2MnX (X=Al, In, Sn): Ab-initio study

Mukesh Chawla

A Dissertation Submitted to
Indian Institute of Technology Hyderabad
In Partial Fulfillment of the Requirements for
The Degree of Master of Science

भारतीय प्रौद्योगिकी संस्थान हैदराबाद
Indian Institute of Technology Hyderabad

Department of Physics

Declaration

I declare that this written submission represents my ideas in my own words, and where others' ideas or words have been included, I have adequately cited and referenced the original sources. I also declare that I have adhered to all principles of academic honesty and integrity and have not misrepresented or fabricated or falsified any idea/data/fact/source in my submission. I understand that any violation of the above will be a cause for disciplinary action by the Institute and can also evoke penal action from the sources that have thus not been properly cited, or from whom proper permission has not been taken when needed.

(Signature)

(– Mukesh Chawla –)

(Roll No. PH11M05)

Approval Sheet

This thesis entitled **'Electronic, Magnetic and Fermi Surface properties of Cu_2MnX (X=Al, In, Sn): Ab-initio study'** by Mukesh Chawla is approved for the degree of Master of Science from IIT Hyderabad.

Vandana Sharma
VANDANA SHARMA, IIT-H

-Name and affiliation-

Examiner

(J. Suryanarayana)

-Name and affiliation-

Examiner

(V. KANCHANA)

-Name and affiliation-

Adviser

-Name and affiliation-

Co-Adviser

-Name and affiliation-

Chairman

Acknowledgements

The success and final outcome of this project required a lot of guidance and assistance from many people and I am extremely fortunate to have got this all along the completion of my project work. I have completed it because of such guidance and assistance. I would not forget to thank them.

First of all, I respect and thank **Dr. V. Kanchana**, for giving me an opportunity to do this project work for my 'Master of Science Degree' and providing me all support and guidance which made me to complete the project on time . I am extremely grateful to her for providing such a nice support and guidance.

I am extremely grateful to the Head of Physics Department, **Dr. Anjan K. Giri** for providing excellent facility and nice atmosphere for completing my M.Sc. course.

I owe my profound gratitude to the Research Scholars **Swetarekha Ram, Vijay Kumar Gudelli, G. Shwetha and P. V. Sreenivasa Reddy**, they took keen interest in my project work and guided me all along, till the completion of my project work by providing all the necessary information required for this.

I am thankful to and fortunate enough to get constant encouragement, support and guidance from all the Faculty of Department of Physics.

Also, I would like to extend my sincere regards to all the non-teaching staff of Department of Physics for their support.

Mukesh Chawla

Abstract

The band structure, density of states, Fermi surface (FS) topology and vibrational properties of the ferromagnetic Heusler alloys, Cu_2MnX (X = Al, In, Sn) have been studied using the first principles electronic structure calculation at ambient as well as under compression. The major

contribution to the total magnetic moment arises from the Mn atom with adequate exchange splitting as revealed from the calculated local magnetic moment as well as from the density of states plots. The Fermi surface topology is found to be similar for the majority band for all the compounds and remain unaltered under compression, where we have seen the linear variation of the density of states ($N(E_F)$) at the Fermi level, whereas the FS topology change is observed in the minority spin band with non-monotonic variation of the $N(E_F)$. Apart from this, under compression at nearly $V/V_0=0.75$, we have seen the Fermi surface topology of the minority spin of Cu_2MnSn to change drastically resembling the majority band Fermi surface. From the phonon dispersion relation, we find a lattice instability in the case of Cu_2MnSn with negative slope around Γ point at ambient as well as under compression and this might induce the anomalous behavior observed in the Fermi surface topology, whereas for other compounds we have found the positive slope at the same point with all positive frequency under all compression, ensuring the dynamical stability of these compounds.

Contents

Chapter 1

Introduction

With the advent of technology and advanced studies with electron spin, an intrinsic property of elementary particle, it is possible to explore various new properties, by virtue of its nature such that it can align itself either parallel or antiparallel to applied magnetic field, like half-metallicity, storage data in memory devices and many more, which maps to a new industry known as spintronics and many new materials are found promising with spintronic applications. Hence it is quite interesting and mandatory to focus our research in search of such materials and one such class of materials are the famous Heusler alloys.

Heusler alloys are the promising materials for spintronics application due to Half-metallic behavior**,** because the existence of a gap in the minority-spin band structure leading to 100% spin polarization of the electron states at the Fermi level and makes these systems attractive for applications in the emerging field of spintronics. Besides this, some Heusler compounds are magnetic in the martensitic phase, and exhibit magnetic shape memory (MSM) effect. The MSM alloys are of great interest as promising smart materials for future technological applications. They can be used as sensors and actuators in different fields of applications. In 1903, Heusler [1] reported that the addition of *sp* elements (Al, In, Sn, Sb or Bi) turn Cu-Mn alloy into a ferromagnetic material even though the alloy contains none of the ferromagnetic elements.

Heusler alloys are ternary intermetallic compounds with basic formula X_2YZ, where X, Y are transition metals, X can be 3d ,4d or 5d element like Co, Ni, Cu etc., Y=Mn, Fe, Cr, etc. and Z=Al, In, Sn, Sb, Si, Ga, Ge and As. X_2YZ type Heusler alloys are formed by the combination of the metallic element of rock-salt like "YZ" structure, where X is occupied in every tetrahedral void. In our present study we have analyzed the electronic structure of the Cu based Heusler alloys Cu_2MnX, where X = Al, In, and Sn. The Cu_2MnAl, is the first compound of Heusler family which show soft magnetic behavior and possess Curie temperature of about 600 K [2]**.** Previous studies on Cu_2MnAl reveal a rare combination of ferromagnetism and structural phase transition from a cubic high-temperature phase into a tetragonal and less symmetric low-temperature phase. The structural properties of Cu_2MnAl have been studied by Robinson et. al [3], where the authors have found the Heusler phase to be unstable when mechanically milled over extended periods. It was also reported that the perfect $L2_1$ order for Cu_2MnAl cannot be achieved after optimum preparation. Cu_2MnAl was found to be decomposed into Cu_3MnAl and Cu_2Al_4 phases above 600 K and this temperature range might vary from 600 to 790 K as per the different studies. To understand the electronic, magnetic and dynamical stability of the Cu_2MnX (X = Al, In, Sn), we have studied the electronic structure, Fermi surface and vibrational properties of all the above Cu_2MnX compounds. The lattice instability is seen in some of the Ni based Heusler alloys, where the authors have reported the same due to an unusual behavior of the optical modes. In addition the phonon instability in Ni_2MnGa was explained due to the Fermi surface nesting. So in this present work we have studied the dynamical stability of all the compounds and find a lattice instability in Cu_2MnSn, at ambient and under compression. The

Fermi surface topology is found to change for the minority spin band of all these investigated compounds under compression. To accomplish this, **Density functional theory (DFT)**, a quantum mechanical modeling method is used, which basically used to investigate the electronic structure (principally the ground state) of many body system, in particular atoms, molecules, and the condensed phases.

The rest of the thesis is organized as follows: In chapter 2 we discuss about the theoretical methods which are necessary to perform the calculations. In chapter 3 we discuss about the computational details, which we used to calculate the properties of these compounds. Results and discussion are explained in the chapter 4 and finally chapter 5 summarizes the results with conclusions.

Chapter 2
Theoretical Background

The fundamental postulates of quantum mechanics assert that microscopic system are described by 'wave function' that completely characterize all the physical properties of the system called observables of various operators defined in quantum mechanics.

Consider a many body system having, P nucleons of charge Z_I at position R_I for n=1, 2…..P and N electrons at position r_i for i=1, 2...N. The main interest is to find approximate solution of non-relativistic time independent Schrödinger equation.

$$\mathbf{H}|\Psi\rangle=\mathbf{E}|\Psi\rangle$$

Many body wave function is of form $\Psi \equiv \Psi\ (\mathbf{R_1, R_2}\ldots\ldots\mathbf{R_P; r_1, r_3}\ldots\ldots\ldots\mathbf{r_N})$ and **E** is the total energy of the system. The Hamiltonian H consists of following.

H=

Where R = $\{\mathbf{R}_I\}$, $I = 1 \ldots P$, is a set of P nuclear coordinates, $\mathbf{r} = \{\mathbf{r}_i\}$, $i = 1 \ldots N$, is a set of N electronic coordinates. Z_I and M_I are the *nuclear* charges and masses, respectively and e amd m are electron charge and mass respectively. It includes kinetic energy (K.E) of all nucleus and electron, the inter nuclei repulsion energy, electron-electron repulsion energy and nuclei-electron attraction energy. In operator form we can write

$$\mathbf{H}=\mathbf{T_n} + \mathbf{T_e} + \mathbf{V_{nn}} + \mathbf{V_{ee}} + \mathbf{V_{en}}$$

$$\mathbf{H}\ \Psi_\mathbf{i}(\mathbf{r,R}) = \mathbf{E_i}\Psi\ (\mathbf{r,R})$$

Electrons are fermions, and the total electronic wave function must be anti-symmetric with respect to exchange of two electrons. Nuclei can be fermions, bosons or distinguishable particles, according to the particular problem under consideration. All the ingredients are perfectly known

and in principle, all the properties can be derived by solving the many-body Schrodinger equation:

Although this equation is exact within the non-relativistic regime, it is not possible, except for trivially simple cases to solve it. Consequently the many-body wave function is a complicated mathematical object that incorporates the effects of correlation, preventing the separation of the electronic degrees of freedom into single-body problems. Thus we must search for approximations that render the Schrödinger equation tractable to numerical solution, while retaining as much of the key physics as is possible.

2.1 Approximation to solve the Many-Body Problem:

2.1.1 Born–Oppenheimer Approximation:

$$\Psi(\mathbf{R}, \mathbf{r}) = \phi(\mathbf{R}, \mathbf{r})\, \chi(\mathbf{R})$$

Since the electrons are much lighter than the nuclei by three orders of magnitude, makes nucleus almost immobile with reference to electrons. This can be exploited by treating the wave function in separable form, as

Where $\chi(\mathbf{R})$ is a nuclear wave function and $\phi(\mathbf{R}, \mathbf{r})$ is an electronic wave function that depends parametrically on the nuclear positions. Besides this, we can neglect the term K.E. of nuclei and consider the term nuclear-nuclear interaction as constant, so our Hamiltonian **H** reduces to

$$H=$$

2.1.2 Hartree-Fock Approximation:

Electrons are *independent*, and interact only via the mean-field Coulomb potential.

Hartree took a different approach to consider the interacting electrons via their own e-e electrostatic interaction and electron-nucleus electrostatic interaction. He thought that whole system can be assume as ‘independent particles/electrons’ and interacting only through mean field coulomb potential. This leads to

$$\phi(\mathbf{r}_1, \mathbf{r}_2, \mathbf{r}_3 \ldots\ldots\ldots \mathbf{r}_N) = \phi(\mathbf{r}_1)\, \phi(\mathbf{r}_2)\, \phi(\mathbf{r}_3) \ldots\ldots\ldots \phi(\mathbf{r}_N)$$

i.e. electrons are independent. This yields one electron Schrödinger eq.

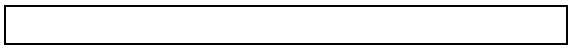

Where V(r) is the potential in which the electrons move, this includes, both the nuclear and electron interaction.

And the mean field arises from the other N-1 electrons. We smear the other electrons out into a smooth negative charge density ρ (**r'**) leading to a potential of the form

Where $\rho(\mathbf{r'}) = \sum_i |\phi(\mathbf{r})|^2$

Although these *Hartree* equations are numerically manipulable via the self-consistent field method, it is not surprising that such a crude approximation fails to capture elements of the essential physics. Since the Pauli Exclusion principle demands that the many-body wave function be anti-symmetric with respect to interchange of *any* two electron coordinates, *e.g.*

. $$\phi(\mathbf{r_1}, \mathbf{r_2}, \ldots\ldots\ldots \mathbf{r_N}) = -\phi(\mathbf{r_2}, \mathbf{r_1}, \ldots\ldots\ldots \mathbf{r_N})$$

This cannot be satisfied by a non-trivial wave function of the independent electron wave function form. This *exchange* condition can be satisfied by forming a Slater determinant of single-particle orbitals

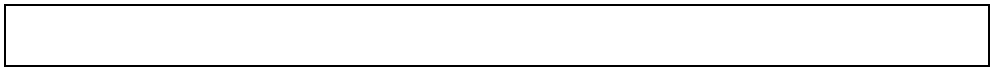

Where *A* is an anti-symmetrizing operator, *i.e.* it ensures that all possible anti-symmetric combinations of orbitals are taken. Again, this decouples the electrons, leading to the single-particle *Hartree-Fock* equations of the form

The last term on the left-hand side is the *exchange* term, this looks similar to the direct Coulomb term, but for the exchanged indices. It is a manifestation of the Pauli Exclusion principle, and acts to separate electrons of the same spin. The exchange term adds considerably to the complexity of these equations.

The Hartree-Fock equations deal with exchange exactly, however, the equations neglect more detailed correlations due to many-body interactions. The effects of electronic correlations are not negligible; indeed the failure of Hartree-Fock theory to successfully incorporate correlation leads to one of its most celebrated failures. The requirement for a computationally practicable scheme that successfully incorporates the effects of both exchange and correlation and leads us to consider the conceptually simple and elegant **Density Functional Theory.**

2.2 Density Functional Theory:

DENSITY FUNCTIONAL THEORY (DFT), is a powerful formulation of many body quantum mechanics, which states that the ground state properties of a quantum many particle system depends only on density. In particular, the ground state density is found by minimizing the energy functional, whose value at minimum also gives the ground state energy. The electron density is defined as

$$\rho(\mathbf{r}) = N \int \ldots\ldots\ldots \int |\Psi(\mathbf{r}_1, \mathbf{r}_2, \ldots\ldots\ldots\ldots \mathbf{r}_N)|^2 \, d\mathbf{r}_1 \, d\mathbf{r}_2 \ldots\ldots d\mathbf{r}_N$$

$\rho(\mathbf{r})$ determine the probability of finding any of the N electrons within the volume element $d\mathbf{r}_1$ but with arbitrary spin, while the other N-1 electrons have arbitrary spin and position in the state represented by Ψ. $\rho(\mathbf{r})$ is a non-negative function of only the three spatial variables which vanish at infinity and integrate to total number of electrons

$$\rho(\mathbf{r} \quad \infty) = 0 \text{ and}$$

$$\int \rho(\mathbf{r}) \, d\mathbf{r} = N$$

2.3 Thomas Fermi Model:

The original density functional theory of quantum mechanics is the idea drawn from Thomas [4] and Fermi [5] proposed in 1927. Although their approximation is not accurate enough for present day electronic structure calculations, the approach illustrate the way to density functional theory. In the original Thomas–Fermi method, the K.E. of electrons is approximated as an explicit functional of density, idealized as non-interacting electrons in the homogenous gas with the density equal to the local density at any given point. Both Thomas and Fermi neglected the

exchange and correlation among the electrons; however this was extended by Dirac in 1930, who formulated the local approximation for exchange still in use today. This leads to the energy functional for the electrons in an external potential $V_{ext}(r)$.

Extension to account for the effect of inhomogeneity have been proposed by many people, known as the Weizsacker correction, but more recent work has found the correction to reduce .

The attraction of DFT theory is evident by the fact that one equation for density is remarkably simpler than the full many body Schrödinger equation that involves 3N degree of freedom for N electrons. The Thomas Fermi approach starts with approximation that are too crude, missing basic physics, such as shell structure and binding of molecules, thus it falls short of the goal of a useful description of electrons in matter.

2.4 Hohenberg- Kohn Equations:

Hohenberg, Kohn and Sham established a theoretical basis for justifying the replacement of the many body wave function by one-electron orbitals [6, 7, 8]. They used two fundamental theorems which leads to modern density functional theory, an alternative approach to deal with many body problem in electronic structure theory.

The charge density is a distribution of probability, i.e. $\boldsymbol{\rho(r_1)d^3r_1}$ represents, in a probabilistic way, the number of electrons in the infinitesimal volume $\boldsymbol{d^3r_1}$. This applies to any system of interacting particles in an external potential $V_{ext}(r)$, including any problem of electrons and fixed nuclei, where the Hamiltonian can be written as H= T + V + U

Where T is K.E., U is the interaction energy.

2.4.1 Hohenberg theorems:

First theorem: "For any system of interacting particles in an external potential $V_{ext}(r)$, the total energy, is a unique functional of the electron density $\rho(r)$".

Second theorem: "A universal functional for the energy E[n] can be defined in terms of density. The density that minimizes the total energy is the exact ground state density".

2.5 Kohn-Sham equations:

Later Kohn and Sham provided [6] a workable computational method based on the following result.

For each interacting electron system, there is a local potential V_{ks}, which result in a density ρ equal to that of interacting system. A lot of work was done to find T[n], V_{ee}[n] [Thomas, Fermi, Slater, Dirac etc], however the most successful approach come back to an 'exact expression' for the kinetic energy 'T', by re-introducing one body orbitals. To do that, Kohn-Sham introduced a fictitious equivalent system of non-interacting electrons under the action of an effective potential V_{eff} generating the same density $\rho(r)$ of the real system.

.

$$\rho(\mathbf{r}^2 \qquad (1)$$

and an orbital dependent exchange charge density, ^{HF} for i^{th} orbital

$$\rho_i^{HF}(\mathbf{r},\mathbf{r'}) = \sum_{j=1 \text{ to } N} \frac{\phi^{\star}_j(\mathbf{r'})\,\phi_i^{\star}(\mathbf{r'})\;\phi_i^{\star}(\mathbf{r})\,\phi_i(\mathbf{r})\;\delta_{si,sj}}{\phi_i^{\star}(\mathbf{r})\,\phi_i(\mathbf{r})}$$

This density involves a 'spin' dependent factor which couples only (i, j) with the same spin coordinate (s_i, s_j). With these defined charge densities, it is possible to define corresponding potentials, the coulomb or Hartree potential,$V_{H,}$ and is defined as

(2)

and an exchange potential can be defined as

This combination results in the following Hartree- Fock equation

Once the Hartree–Fock orbitals have been obtained, the total Hartree-Fock electronic energy of system, E_{HF} can be obtained from

Thus the Kohn-Sham energy functional is formally written as

$$H_{KS} = \qquad (3)$$

Where the effective potential is defined as for an one-electron potential, i.e.

$$V_{eff} = V_N(\rho) + V_H(\rho) + V_{xc}(\rho)$$

E_{HF} is not a sum of the Hartree- Fock orbitals energy E_i. The factor of one half in the e-e terms arise since the e-e interactions have been double counted in the coulomb and exchange potentials. The Hartree- Fock Schrödinger equation is slightly more complex than the Hartree equation.

Note that in contrast with Equation

V_{xc} is now without an index, as it is only for one electron. Also note the dependence of each potential term on the charge density ρ, which is implicitly defined from the set of occupied energies Ψ_i, i=1, 2….N of the equation (3) by equation (1). The energy term associated with the nuclei – electron interaction is $<V_N|\rho>$, while that of e-e interaction is $<V_H|\rho>$, where V_H is Hartree potential

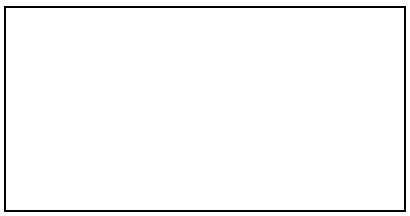

The Kohn- Sham energy functional is of following form

And the Konh-Sham equation for electronic structure of matter is given as

$$+ V_N(r) + V_H(r) + V_{xc}[\rho(r)]) \Phi_i(r) = E_i \Phi_i(r)$$

This equation is usually solved 'self-consistently'. An approximate charge is assumed to estimate the exchange-correlation potential, and this charge is used to determine the Hartree potential form of Eq (2). These approximate potentials are inserted in Kohn-Sham equation and the total charge density is determined as in Eq (1). The 'output' charge density is used to construct new exchange correlation and Hartree potentials. The process is repeated until the input and output charge density or potentials are identical within some tolerable limit. Once self-consistency is achieved, a solution of the Kohn-Sham equation is obtained, and the total energy can be written as

$$E_{KS} = = \sum E_i - \tfrac{1}{2} \int \rho(r) V_H d^3r - \int \rho(\mathbf{r}) E_{xc}[\rho(\mathbf{r})] - V_{xc}[\rho_{(r)}] d^3r$$

$$\text{i=1 to N}$$

The algorithm of this self-consistent calculation is shown in **Fig 2.1.**

2.6 Local Density Approximation (LDA):

A key contribution by Kohn and Sham is the local density approximation, which is used to approximate the exchange energy and is expressed as

$$E_x[\rho(r)] = \int \rho(r)\varepsilon_x(\rho(x))d^3r$$

Where $\varepsilon_x[\rho]$ is the exchange energy per particle of an uniform gas at a density ρ. The exchange potential is replaced by a potential determined from derivative of $E_x[\rho]$

$$+ V_N(r) + V_H(r) + V_{xc}(\rho(r)) = E_i \Phi_i(r)$$

$V_{xc}[\rho]=$ and the corresponding exchange potential is V_x.
The expression for either of these quantities is unknown, from Hartree –Fock theory one can show that the exchange energy is given by

Which is the Hartree Fock expression for the exchange energy of a free electron gas. In this expression, **k** is the wave vector for a free electron; it can be related to the momentum by $p = \hbar k$. The highest wave vector is given by k_F, where the Fermi energy is given by $E_F = \hbar^2 k_F^2 / 2m$. One can write

$$E_x[\rho] = (3\pi^2)^{1/3} \int [\rho(r)]^{4/3} d^3r$$

.

And its functional derivative

$$V_x[\rho] = -(3\pi^2\rho(r))^{1/3}$$

2.7 Generalized Gradient Approximation (GGA):

As the LDA approximate the energy of the true density by the energy of a local constant density, it fails in the situations where the density undergoes rapid change such as in molecules. An

improvement to this can be made by considering the gradient of the electron density, so called Generalized Gradient Approximation, symbolically it can be written as

$$E_x = E_{xc}[\rho(\mathbf{r}), \rho(\mathbf{r})]$$

This can lead to a large improvement over LDA result.

Some of these are semi-empirical, in that experimental data e.g. atomization energy is useful in their derivation. A commonly used functional are PBE, PW91 functional, due to Perdew-Burke-Ernzerhof parameterization, Perdew and Yan respectively.

Algorithm of Self-Consistent Calculation

Fig. 2.1 Algorithm for self-consistent calculation

Chapter 3

Computational Details

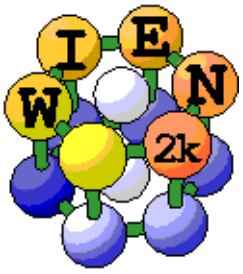

3.1 The LAPW method:

The linearized augmented plane wave (LAPW) method is among the most accurate methods for performing electronic structure calculations for crystals. It is based on the density functional theory for the treatment of exchange and correlation and uses e.g. the local spin density approximation (LSDA). Several forms of LSDA potentials exist in the literature, but recent improvements using the generalized gradient approximation (GGA) are available too. For valence states relativistic effects can be included either in a scalar relativistic treatment or with the second variational method including spin-orbit coupling. Core states are treated fully relativistically. The LAPW method is a procedure for solving the Kohn-Sham equations for the ground state density, total energy, and (Kohn-Sham) eigenvalues (energy bands) of a many-electron system (here a crystal) by introducing a basis set which is especially adapted to the problem [9].

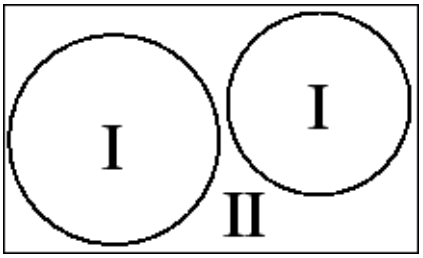

Figure 3.1: **Partitioning of the unit cell into atomic spheres (I) and an interstitial region (II)**

This adaptation is achieved by dividing the unit cell into (I) non-overlapping atomic spheres (centered at the atomic sites) and (II) an interstitial region. In the two types of regions different basis sets are used:

- Inside atomic sphere t of radius R_t a linear combination of radial functions times spherical harmonics $Y_{lm}(r)$ is used (we omit the index t)

Where is the regular solution of the radial Schrödinger equation for energy E_l (chosen normally at the center of the corresponding band with l-like character) and the spherical part of the potential inside sphere t . $_l$ (r, E_l) is the energy derivative of u_l taken at the same energy E_l. A linear combination of these two functions constitute the linearization of the radial function; the coefficients A_{lm} and B_{lm} are functions of k_n determined by requiring that this basis function matches (in value and slope) the corresponding basis function of the interstitial region and $_l$ are obtained by numerical integration of the radial Schrödinger equation on a radial mesh inside the sphere.

- In the interstitial region a plane wave expansion is used

$$\phi_{k_n} = \frac{1}{\sqrt{\omega}} e^{ik_n r}$$

Where $k_n=k+K_n$; K_n are the reciprocal lattice vectors and k is the wave vector inside the first Brillouin zone. Each plane wave is augmented by an atomic-like function in every atomic sphere.

The solutions to the Kohn-Sham equations are expanded in this combined basis set of LAPW's according to the linear variation method

$$\psi_k = \sum_n c_n \phi_{k_n}$$

and the coefficients c_n are determined by the Rayleigh-Ritz variational principle. The convergence of this basis set is controlled by a cutoff parameter $R_{mt}K_{max}$= *6 - 9*, where R_{mt} is the smallest atomic sphere radius in the unit cell and K_{max} is the magnitude of the largest K vector.

3.2 Details of calculation

All the present calculations were performed by using the Full Potential Linearized Augmented Plane Wave (FP-LAPW) method as implemented in the WIEN2k [10, 11] code, within generalized gradient approximation (GGA) for the exchange correlation potential corresponding to the PBE-GGA (Perdew-Burke-Ernzerhof parameterization of the Generalized Gradient Approximation) approximation [12]. For the energy convergence, the R_{MT} (radius of muffin tin spheres) value for each atom was fixed as 2.10 a.u. for Cu atom and Mn atom, 1.95 a.u for Al atom and 2.00 a.u for In atom and Sn atom. The plane wave was expanded with the criterion R_{MT}*K_{max}=7 for all the investigated compounds, where K_{max} is the plane wave cut-off. The potential and charge density were Fourier expanded till G_{max}=12. For the electronic properties like band structure, density of states and Fermi surfaces we have used 32×32×32 k-mesh within Monkhorst-Pack [13] scheme which generates 897 k-points in the irreducible part of the Brillion

zone (BZ). The densities of states (DOSs) were obtained by the modified tetrahedron method. Birch-Murnaghan [14] equation of states was used to fit the total energies as a function of primitive unit cell volume to obtain the Bulk modulus and the equilibrium lattice parameter for all compounds. The three dimensional Fermi surface were drawn using the Xcrysden molecular structure visualization program. The total energy was converged up to 10^6 Ry.

Quantum espresso package [15] has been used for the phonon dispersion. In order to deal with the possible convergence problem for metals, a smearing technique is employed using the Methfessel-Paxton (MP) scheme, with the smearing parameter set to 0.02 Ry for all compounds. For the description of the electron-ion interaction the ultrasoft pseudopotential was used. For the energy convergence we have used the wave function and charged-density cutoffs of 30 Ry and 360 Ry, respectively. Phonons are calculated on an 2×2×2 q- point grid with Brillouin zone integrations on a 32×32×32 Monkhorst-pack-point mesh. The phonon frequencies and atomic displacements were subsequently obtained using the linear response method.

Chapter 4

Results and Discussion

The magnetic properties, band structure, Fermi surface topology and vibrational properties of the ferromagnetic Heusler alloys, Cu_2MnX (X = Al, In, Sn) have been studied using the first principles calculations at ambient as well as under compression.

4.1 Ground state properties:

To calculate the theoretical lattice parameter and bulk modulus for all the investigated compounds, we have used the Birch-Murnaghan [14] equation of states and the values are reported in **Table 4.1** along with the available experimental lattice parameters. The atomic positions are taken as Cu (0.25, 0.25, 0.25), Mn (0.0, 0.0, 0.0), X (0.5, 0.5, 0.5) (X = Al, In, Sn) and the corresponding crystal structure is shown in **Fig. 4.1.**

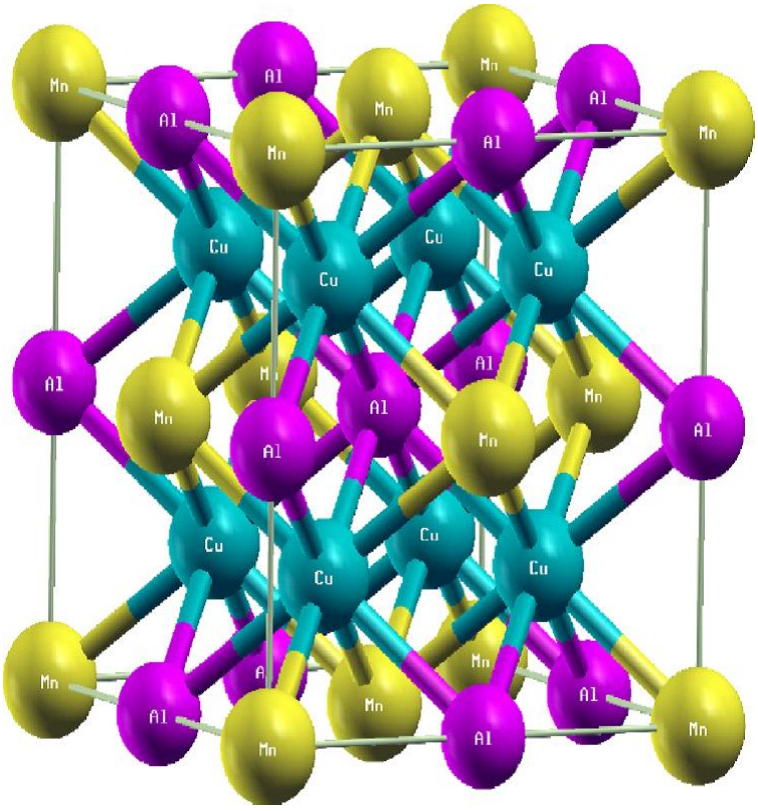

Fig. 4.1 Crystal structure of Cu_2MnX (X = Al, In, Sn).

Table 4.1 Ground state properties of Cu_2MnX (X = Al, In, Sn).

PARAMETERS	Cu_2MnAl	Cu_2MnIn	Cu_2MnSn
a_{exp} (Å)	5.950	6.200	6.170
a_{theo} (Å)	5.925	6.177	6.213
B (GPa)	126.72	108.15	105.36

From the calculated values we have found the maximum error in the lattice parameter to be 0.695 % for Cu_2MnSn and the minimum error of 0.35 % for Cu_2MnIn. The bulk modulus of all the compounds are found to be comparatively high indicating all the compounds to be stiffer, and again the bulk modulus values decrease when X is replaced by Al, In and Sn respectively.

4.2 Magnetic properties, Electronic structure, density of states and Fermi surface:

4.2.1 Magnetic Moment: The calculated total magnetic moments of all the three compounds and the atomic specific magnetic moments are shown in **Table 4.2**, along with the corresponding experimental values. Our calculated magnetic moments for all the compounds agree quite well with the available experimental results. From the **Table 4.2,** we can see that, the Cu_2MnAl has a local magnetic moment of 0.046 μ_B on Cu and 3.34 μ_B on Mn leading to the total magnetic moment of 3.52 μ_B for experimental lattice parameter, indicating the exchange interaction to be more in the case of Mn in comparison to the Cu and is also well evident from the density of states as we discuss later. The scenario is same for rest of the other compound Cu_2MnIn and Cu_2MnSn.

Table 4.2. Calculated and experimental values of total and partial magnetic moments (in μ_B) of Cu_2MnX, X=Al, In, Sn.

COMPOUNDS	TOTAL MAGNETIC MOMENT (μ_B)		PARTIAL MAGNETIC MOMENT (μ_B)		
	EXPERIMENT	CALCULATED	Cu	Mn	X
Cu_2MnAl	3.7	3.52	0.04	3.34	-0.038
Cu_2MnIn	4.0	3.74	0.03	3.53	-0.019
Cu_2MnSn	4.1	3.86	0.05	3.52	-0.0006

4.2.2 Band structure and density of states:

The band structures for the compounds Cu_2MnX (X= Al, In, Sn) are illustrated in **Fig.4.2**, at the corresponding experimental volumes (V_0). Our calculated band structure for Cu_2MnAl is found in good agreement with earlier study of Ref. [16]. It was apparent that the band structures at the vicinity of the Fermi level for all the three compounds Cu_2MnX (X= Al, In, Sn,) are similar in all high symmetry points at zero pressure for the majority spin and the minority spin band, and is well reflected in the Fermi surface, which we discuss in next section. The lowest single valence band at nearly -7 eV in majority as well as in minority spin states are mainly due to s orbital of Al, In and Sn and are well screened and remain insensible by exchange interaction between the two transition metals Cu and Mn. The bands lying close to the Fermi level are the one's arising from the hybridization of Cu-d states and Mn-d states including a minor contribution from p

states of X (X =Al, In, Sn). The majority and minority bands for all the compounds are strongly metallic in nature with comparatively more in minority band for Cu_2MnIn, Cu_2MnSn than the majority band, whereas we have seen the metallization to dominant by majority band for Cu_2MnAl over minority band and is well confirm from the density of states (**Fig. 4.3**). Again when we compare the band structure of In containing compounds with Sn containing compound, we can see the band filling in the case of Cu_2MnSn, due to an electron extra in the case of Sn in comparison with In. The total spin polarized density of states (DOS) for all the investigated compounds are illustrated in **Fig. 4.3**, along with the *l* and *m* projected DOS from each atom. **Fig 4.3,** signifies the strong hybridization between the Cu-d, Mn-d with small contribution of X-p at the vicinity of Fermi level. Apart from this, we can see the exchange splitting between majority and minority spin and crystal field splitting between participating atom's d_{eg} and d_{t2g} orbitals. It is evident that the exchange splitting is dominate in Mn atom when compared to Cu atom, which implies Mn atom to contribute more for the total magnetic moment and it can be seen from the magnetic moment as reported in the **Table 4.2**. In addition, it is also found that the crystal field splitting between d_{eg} and d_{t2g} orbitals of Mn is more than the Cu as shown in **Fig. 4.3**. Our calculated density of states for Cu_2MnAl also agree well with the earlier study of Ref. [17].

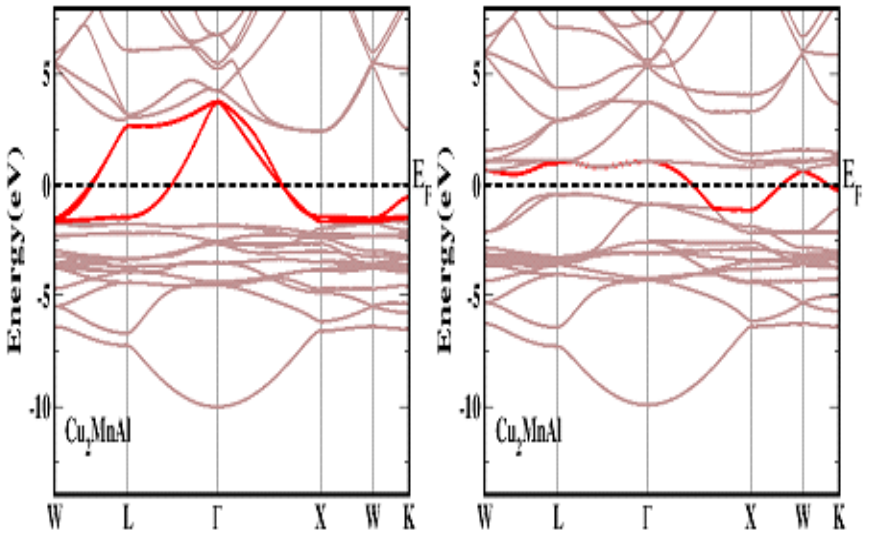

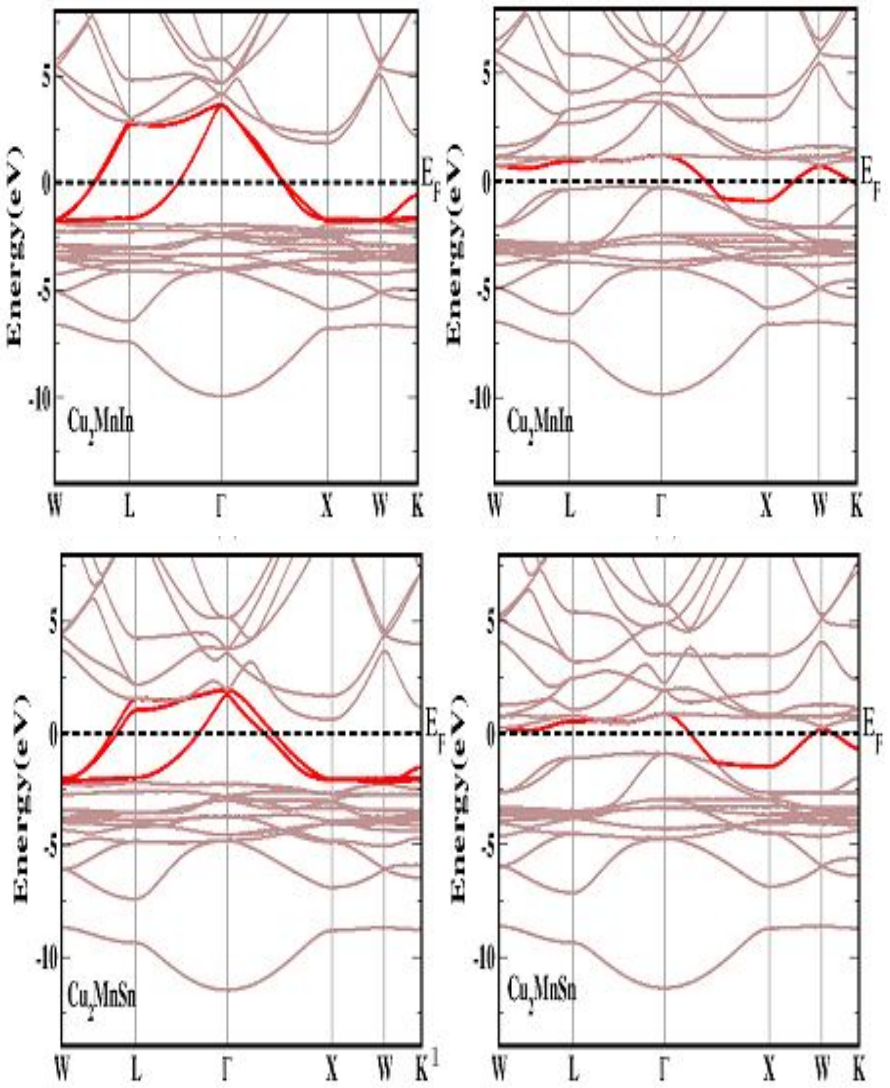

Fig. 4.2: Band structures of Cu_2MnX (X = Al, In, Sn) at ambient, left panel for the majority band and right panel for minority band.

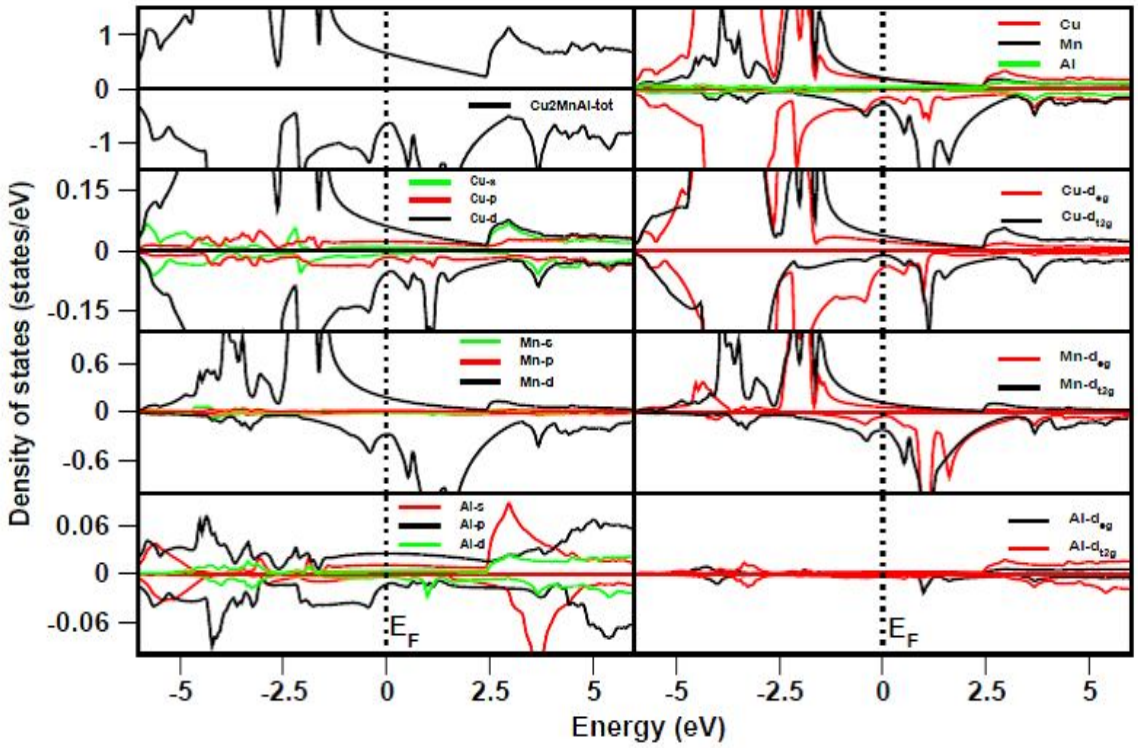
Density of states (states/eV)
Energy (eV)
Cu2MnAl-tot
Cu
Mn
Al
Cu-s
Cu-p
Cu-d
Cu-d$_{eg}$
Cu-d$_{t2g}$
Mn-s
Mn-p
Mn-d
Mn-d$_{eg}$
Mn-d$_{t2g}$
Al-s
Al-p
Al-d
Al-d$_{eg}$
Al-d$_{t2g}$
E$_F$
E$_F$

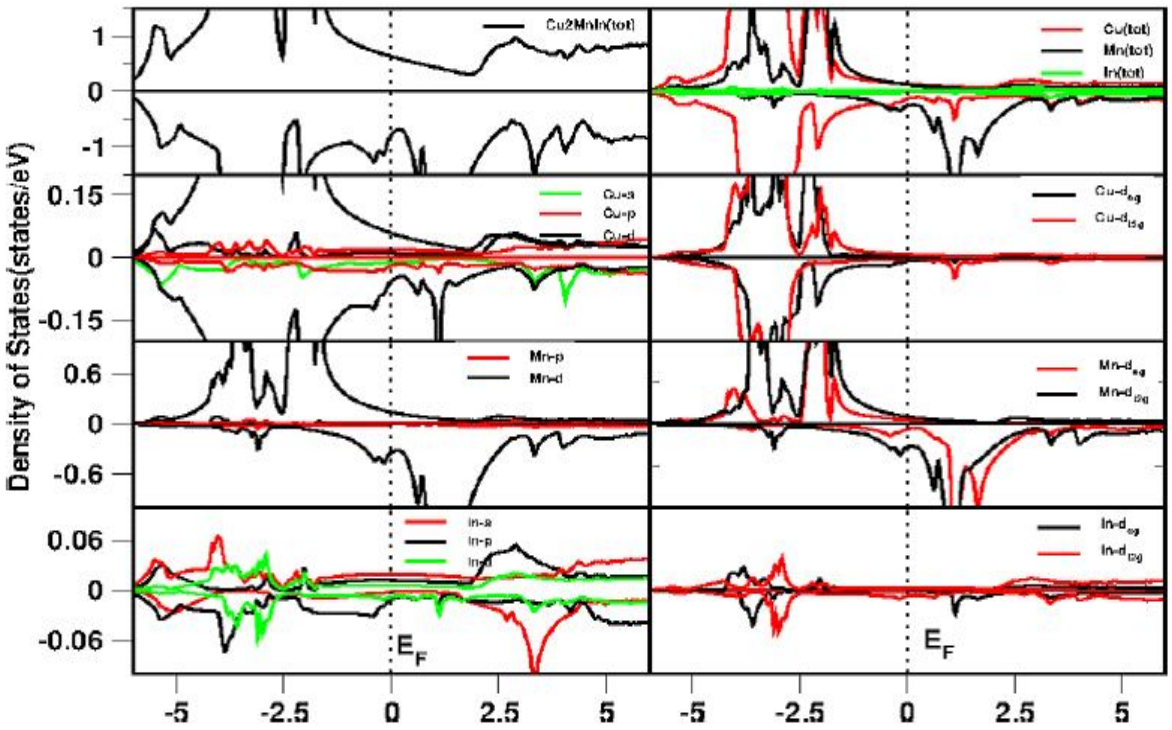
Density of States(states/eV)
Cu2MnIn(tot)
Cu(tot)
Mn(tot)
In(tot)
Cu-s
Cu-p
Cu-d
Cu-d$_{eg}$
Cu-d$_{t2g}$
Mn-p
Mn-d
Mn-d$_{eg}$
Mn-d$_{t2g}$
In-s
In-p
In-d
In-d$_{eg}$
In-d$_{t2g}$
E$_F$
E$_F$

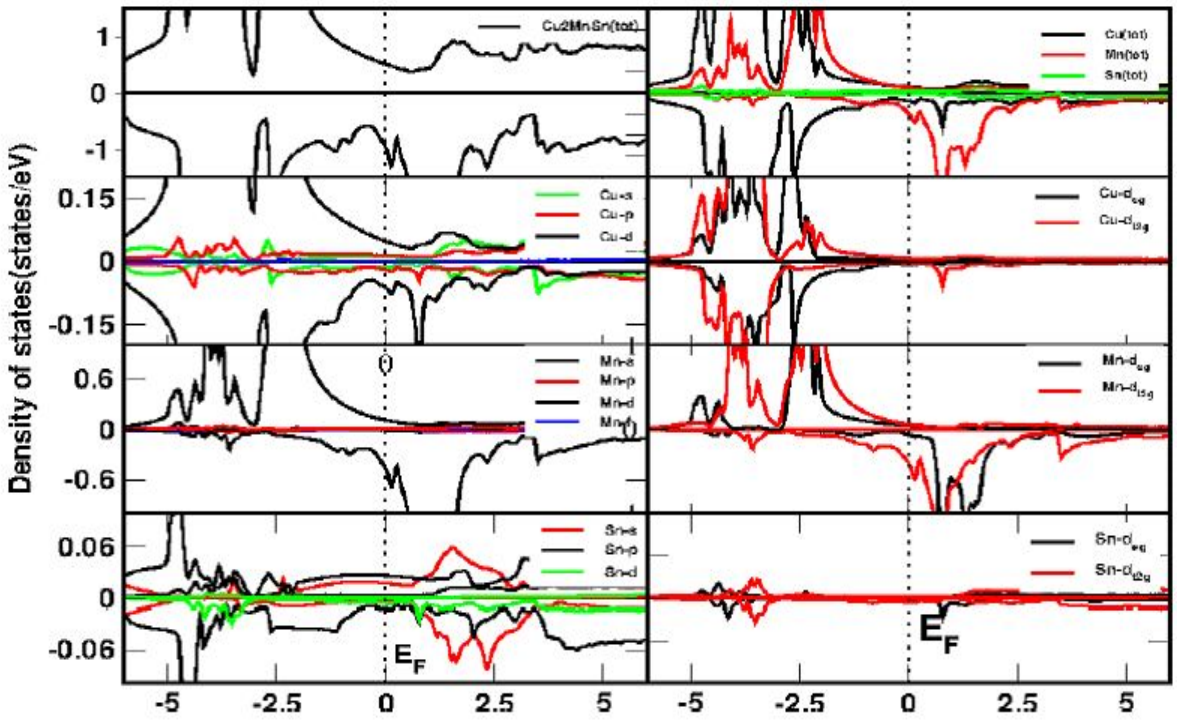

Fig. 4.3: Density of states for Cu_2MnX (X = Al, In, Sn).

4.2.3 Fermi surface:

The Fermi surfaces of all the compounds for majority as well as minority spin are shown in **Fig. 4.4 and 4.5,** respectively. At ambient condition for the majority spin band, we find the Fermi surfaces to be almost similar for all the compounds indicating the strong hybridization of Cu-d and Mn-d orbital. Among all surfaces first Fermi surface for the majority band is hole like centered at Γ-point in the Brillion zone, having a shape of roundish octahedron and second, third Fermi surface have mixed character i.e. hole as well as electron like open sheet and is well evident from the band structure in **Fig. 4.2**, which shows three bands to cross at the corresponding symmetry point on the Fermi level in the majority band for all the compounds. For the minority spin we find two Fermi surface for Cu_2MnAl, and Cu_2MnIn, but for Cu_2MnSn we find only one Fermi surface. We observe Fermi surface to be electron like pocket at X point as well at K point for all the compounds (see **Fig. 4.4**). When we compare the Fermi surface of In and Sn containing compounds we can see the electron pocket to be larger in size for Cu_2MnSn in comparison to the In containing compounds due to band filling, as we discussed earlier in the band structure. Having an extra electron in the case of Sn leads to opening of the electron pocket, which is centralized and closed at X point in minority spin FS for the other compounds as shown in **Fig. 4.5**. Our calculated Fermi surface for Cu_2MnAl is quite similar to earlier report of Ref. [15].

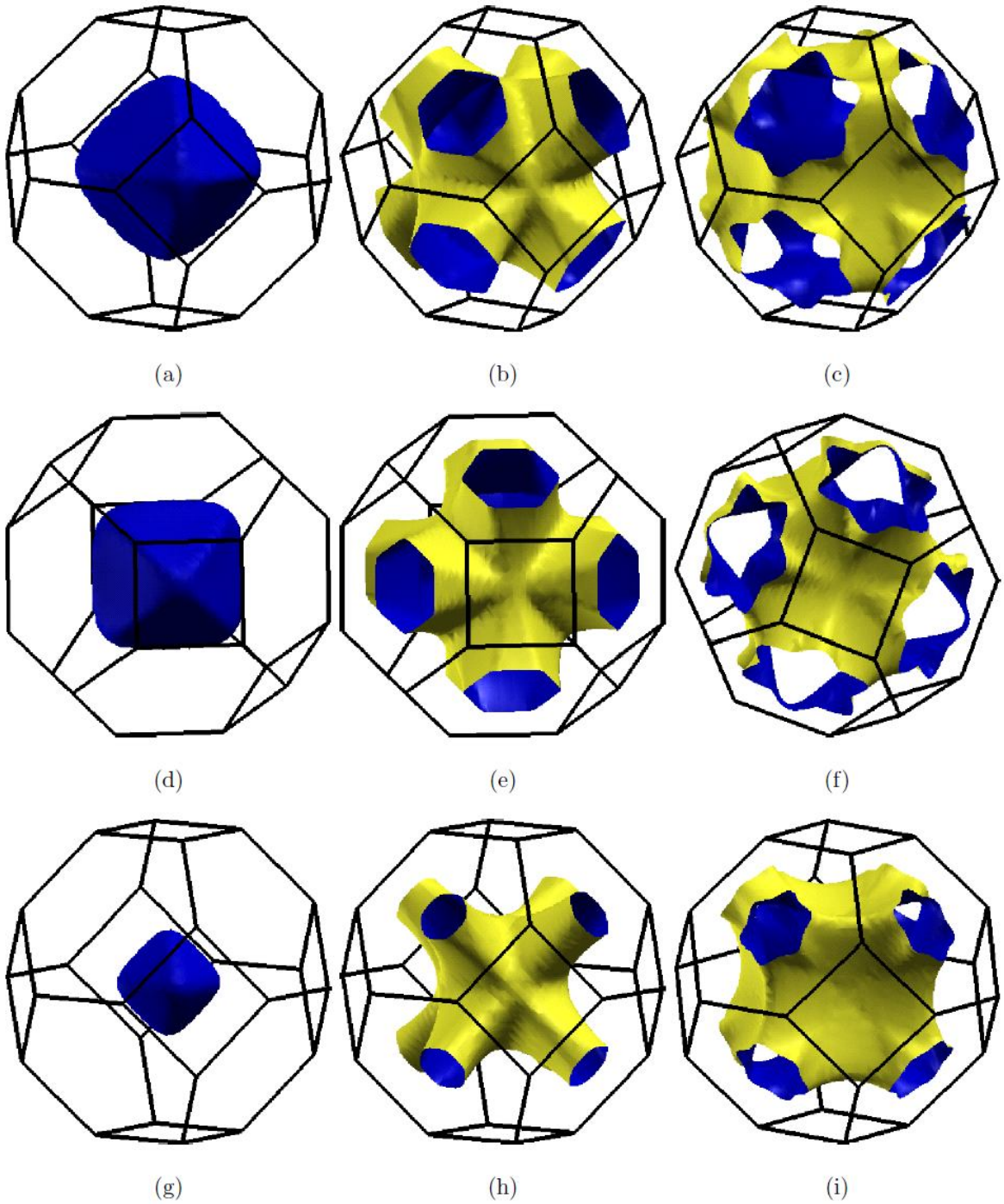

Fig. 4.4: Majority band Fermi surface of Cu_2MnAl (upper panel), Cu_2MnIn (middle panel) and Cu_2MnSn (lower panel)

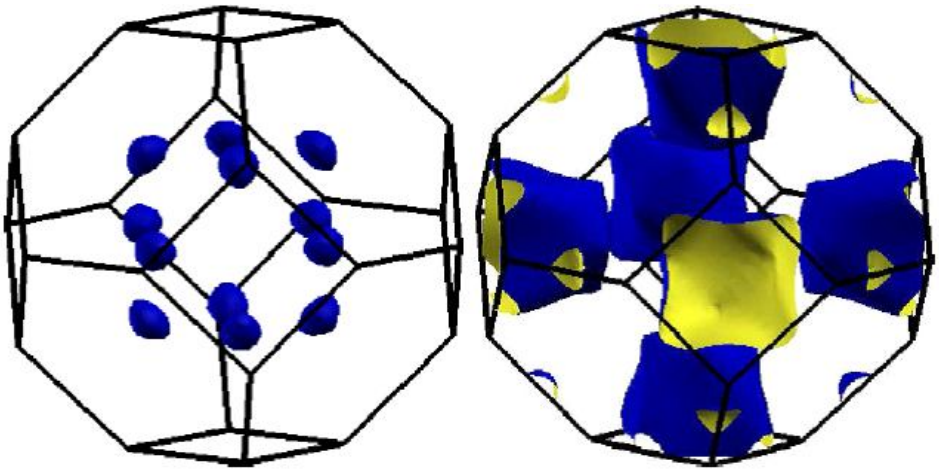

(j)

(k)

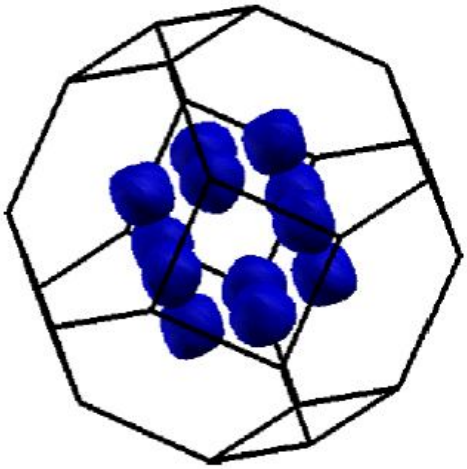

(l)

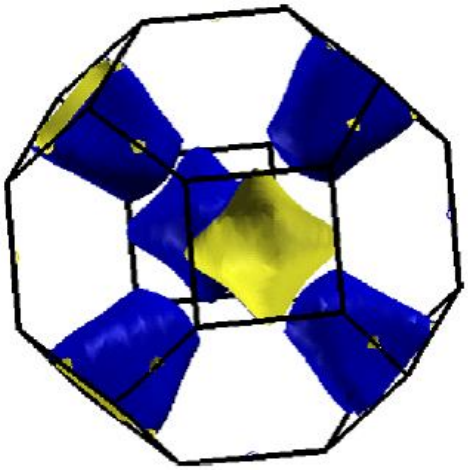

(m)

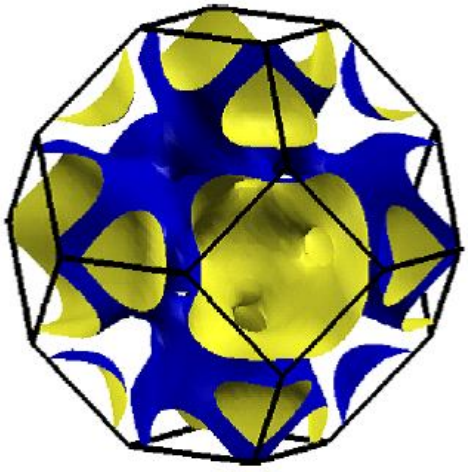

(n)

Fig. 4.5:

Minority band Fermi surface of Cu_2MnAl (upper panel), Cu_2MnIn (middle panel) and Cu_2MnSn (lower panel).

4.3 Effect under compression:

The variation of magnetic moment with the pressure is presented in **Fig. 4.6**, along with local magnetic moments of Cu and Mn site. It is observed that total magnetic moment decreases with pressure. Under compression, magnetic moment is found to be increased for Cu but the overall decrease in the total magnetic moment is mainly due to the Mn atom in all these investigated compounds and is also revealed from this figure. In addition, we have also calculated the DOS under pressure and is plotted in **Fig.4.7,** which indicates that, for majority spin there is no significant change in density of states under compression and the Fermi surface for the same spin are also inert to compression, whereas for minority spin it is the Mn atom which play a vital role in inducing the variation of total density of states but the behavior of Mn atom is different in different compounds. In addition, for all these investigated compounds Cu_2MnX (X = Al, In, Sn) we observe Fermi surface to be unaltered under compression for the majority spin, with the linear variation of the $N(E_F)$ as shown in **Fig.4.7**. But when we analyze the minority band Fermi surface we find the topology to be changed with non-monotonic variation of the density of states. For the minority spin, we observe the first Fermi surface, hole like character for Cu_2MnAl and Cu_2MnIn at Γ point to vanish under compression around $V/V_0 = 0.90$ and $V/V_0 = 0.80$ for Cu_2MnAl and Cu_2MnIn, respectively. The second Fermi surface, which is common in all three investigated compounds, the electron concentration increasing at K and X symmetry points and the Fermi Surface gets merged as shown in **Fig.4.8.** These can be well observed from band structure, **Fig.4.9**, where we can see the band to move down particularly at K symmetry point leading to the increase in the concentration of electron at K symmetry point under compression. Besides this in the case of Cu_2MnSn, the Fermi surface at around $(V/V_0) = 0.80$ shows a strange change, which might be due to an extra valence electron compared to Al and In and might also be due to the presence of lattice instability. First, we have seen a new extra electron like Fermi surface to appear due to dipping of the band down to the Fermi level at symmetry point W (**Fig. 4.8(**e)), and secondly, the complicated surface topology is found to change slowly and looks similar to the Fermi surface of majority spin band FS of Cu_2MnSn, which is well evident from the **Fig 4.4(**h). The corresponding FS under compression are shown in **Fig. 4.8**(d).

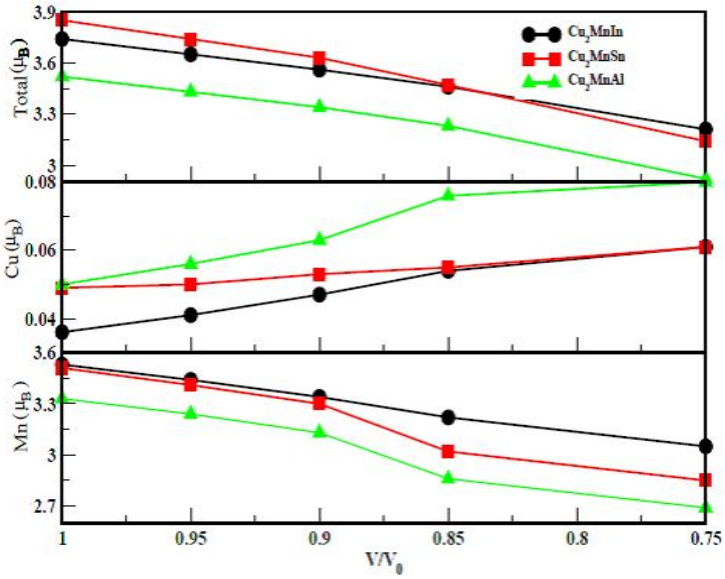

Fig.4.6: Variation of magnetic moment under compression for Cu_2MnX (X = Al, In, Sn).

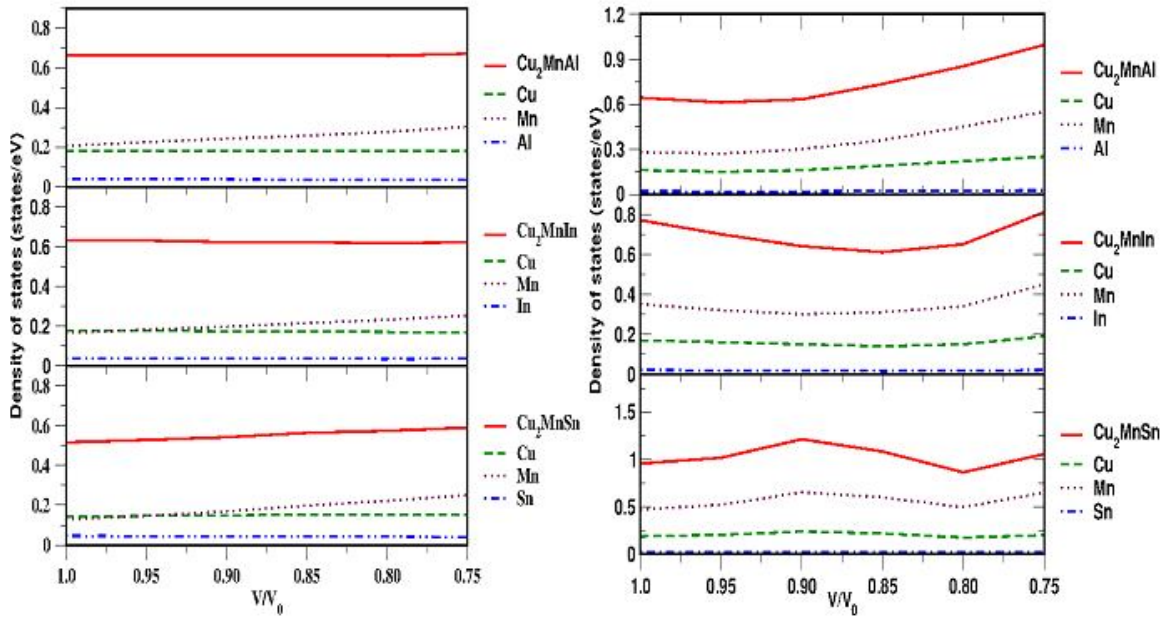

Fig. 4.7: Variation of the total density of states ($N(E_F)$) and the atomic density of states at the Fermi level for Cu_2MnX (X = Al, In, Sn), left panel for majority spin and right panel for minority spin.

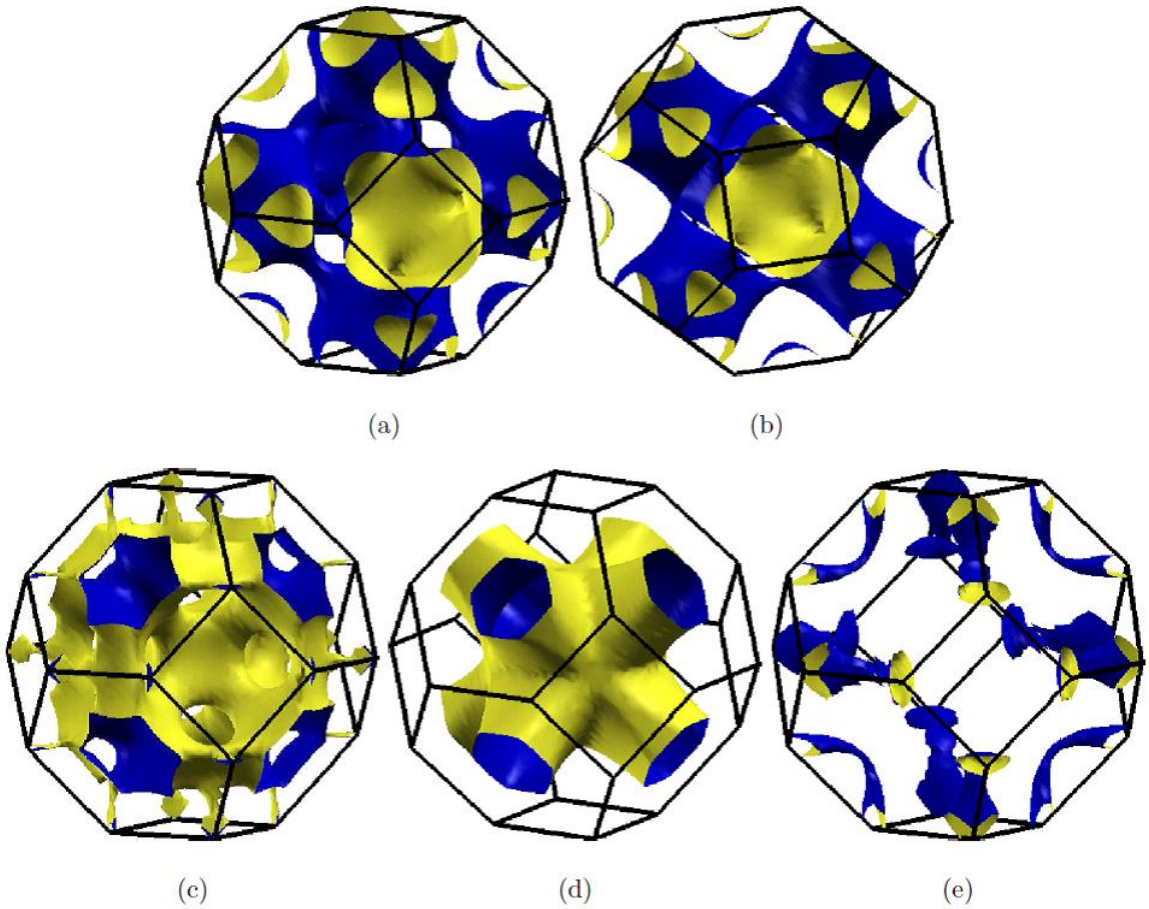

Fig.4.8: Fermi surface under compression (a) Cu_2MnAl at V/V_0=0.9, (b) Cu_2MnAl at V/V_0= 0.8, (c, d) Cu_2MnSn at V/V_0= 0.9 and 0.8 respectively (e) New sheet at V/V_0= 0.8 in Cu_2MnSn.

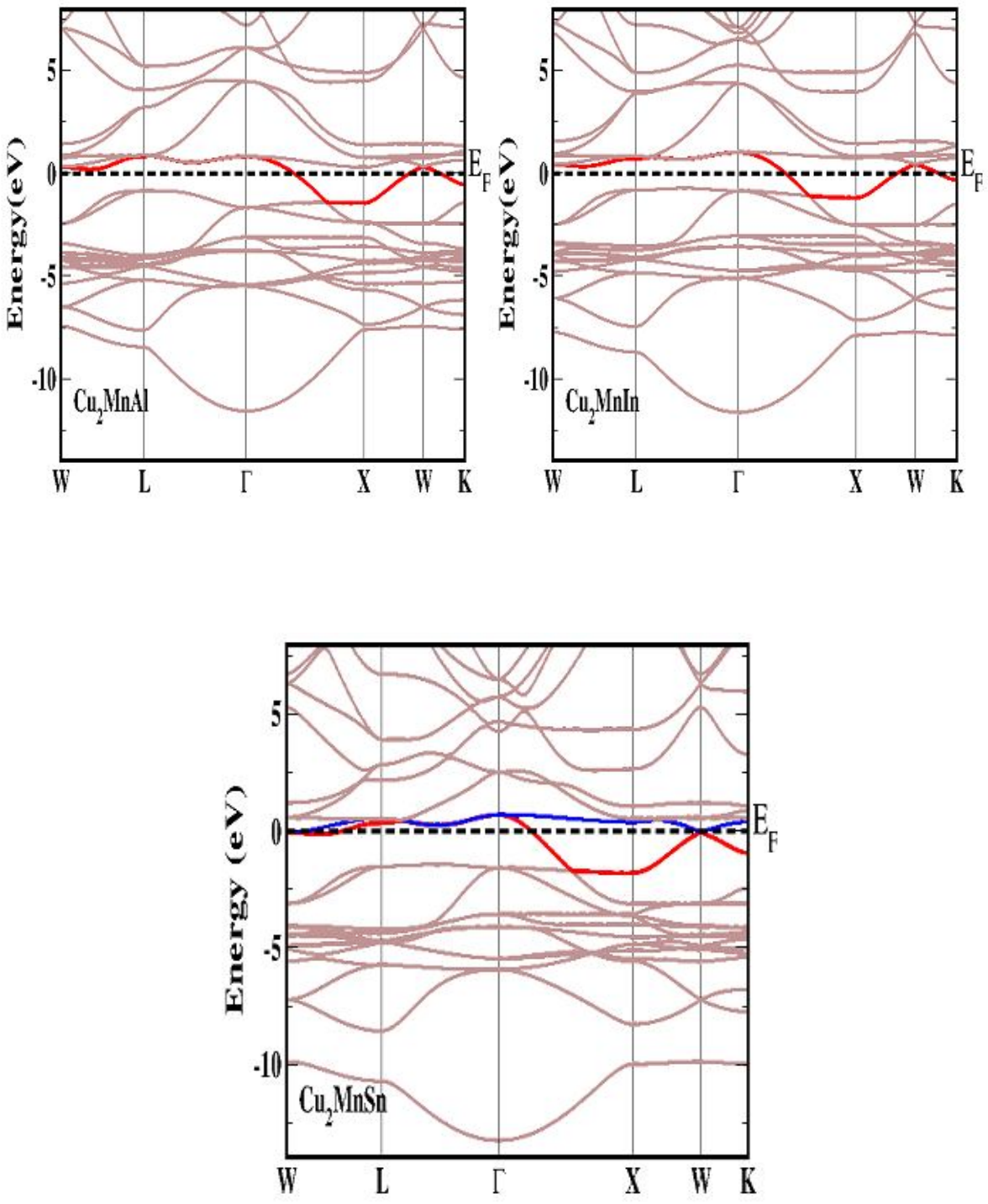

Fig. 4.9: Band structure of Cu_2MnX under compression for minority spin.

4.4 Vibrational properties:

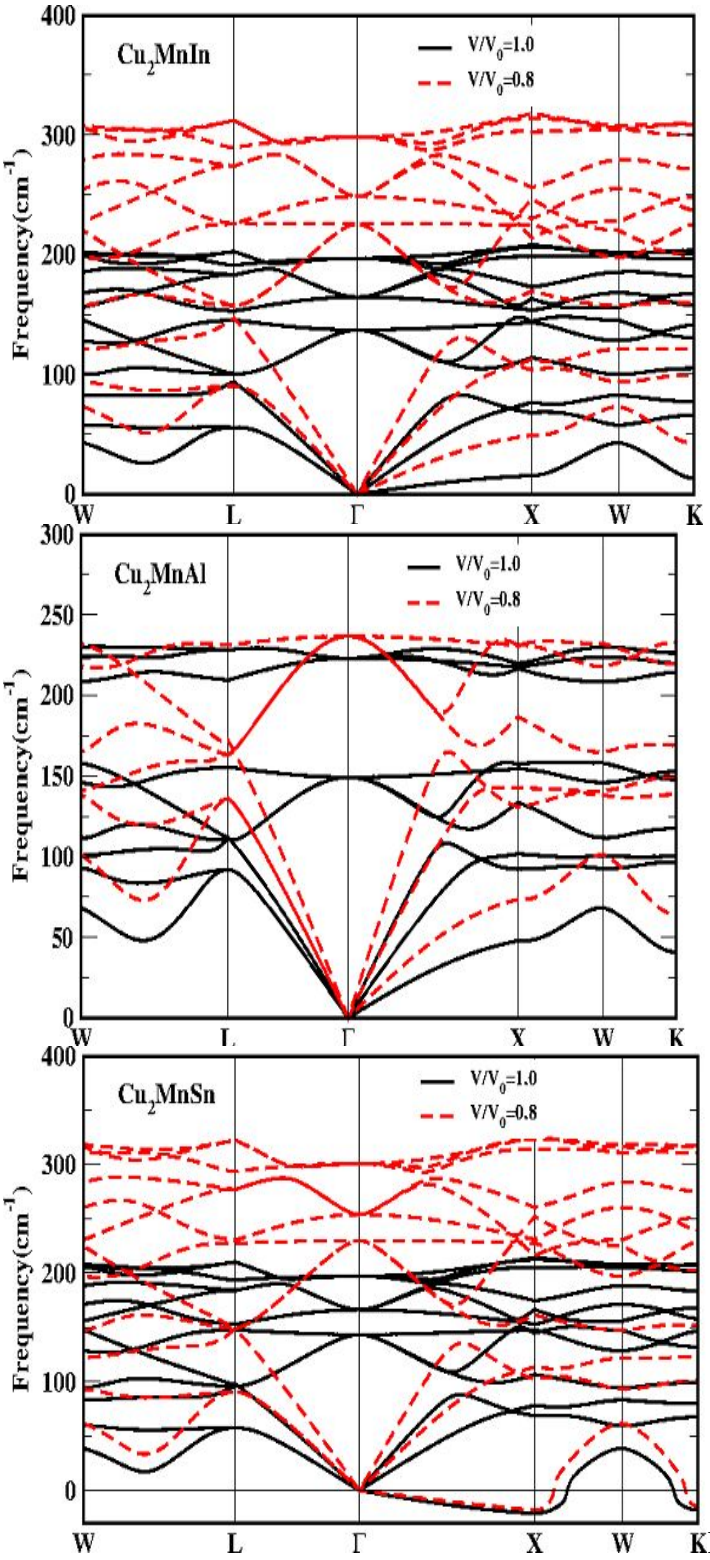

In addition to this we have also calculated the phonon dispersion along the high symmetry direction for all the compounds to ensure the dynamical stability of these compounds. From the calculated dispersion plots as shown in **Fig.4.10**, we find the imaginary mode with negative slope only in the case of Cu_2MnSn, indicating the compounds to be dynamical unstable at ambient as well as under compression,

whereas Cu_2MnAl and Cu_2MnSn is found to be dynamically stable at ambient as well as under compression. In previous study the $L2_1$ phase of the Cu_2MnAl was speculated to be unstable, but we find the Heusler phase to be stable in the case of Cu_2MnAl, which further needs experimental clarification. The lattice instability in the case of the Cu_2MnSn might induce the observed unusual Fermi surface topology change in the minority spin as we discussed in the previous section.

Fig. 4.10 Phonon dispersion along the high symmetry directions for Cu_2MnX (X = Al, In, Sn) at ambient and under compression.

Chapter 5

Conclusion

The first principles study of electronic structure, density of states, Fermi surface and vibrational properties of the Cu_2MnX (X = Al, In, Sn) has been performed with full potential linearized augmented plane wave method at ambient as well as under compression. The exchange splitting is found to be more in the case of the Mn, resulting in the major contribution towards the total magnetic moment from the Mn and is also well evident from the density of states. The observed strong hybridization of Cu-d and Mn-d orbital in all compounds is reflecting well in the majority band FS, where we have found the majority FS topology to be almost similar, whereas under compression at nearly $V/V_0 = 0.75$, the minority band Fermi surface of Cu_2MnSn is found to be similar to that of majority band of Cu_2MnSn and which might be due to the lattice instability of Cu_2MnSn. From the phonon dispersion relation we have found the lattice instability in the case of the Cu_2MnSn with negative slope at Γ at ambient as well as under compression, whereas for other compounds we have found the positive slope at the same point with all positive frequency

under all compression. The Fermi surface topology is found to be unaltered for all the investigated compounds in the majority band under compression, which correlates well with the linear variation of the density of states at the Fermi level. At the same time the Fermi surface topology change is observed in the minority spin band with non-monotonic variation of the $N(E_F)$.

Bibliography

[1] Heusler F., Starck W., Haipt E., Verh Dtsch Phys. Ges (1903) 5, 219.

[2] Do Bang, Nguyen Huy Dan, Nguyen Anh, Nguyen Xuan Phu, Journal of Magnetism and Magnetic Material (2007) 310, 48-50.

[3] Robinson J. S., Mccormick P. G. and Strect R., J.Phys Condense Matter (1995) 7, 4259-69.

[4] Thomas L.H., 'the calculation of atomic fields' Proc. Cambridge Phil. Roy. Soc (1927) 23, 542-548.

[5] Fermi E., 'un metdo statistic per la determinazione di alcune priorieta dell' atome'', Rend. Accad. Naz. Linci (1927) 6, 602-607.

[6] Hohenberg P. and Kohn W., Inhomogeneous electron gas, Phys. Rev. B (1964) 136, 864-871.

[7] Kohn W. and Sham L. J., Self consistent equations including exchange and correlation effect, Phys. Rev. A (1965) 140, 1133-1138.

[8] Lundqvist S. and Marc N. H., 'Theory of the Inhomogeneous Electron Gas', Plenum, (1983).

[9] Adapted from the Wien2k manual.

[10] Blaha P., Scwarz K., Sorantin P. I., Tricky S. B., Comput. Phys. Commun (1990) 59, 399.

[11] Blaha P., Scwarz K., Madsen G. K. H., Kvasnicka D., Luitz J., In: Schwarz K, editor. WIEN2k, an augumented plane wave plus local orbital programe for calculating crystal . properties. Austria:Tech. Techn. Universit¨at wien, Austria, (2001).
[12] Perdew J. P., Burke K., Ernzerhof M., Phys. Rev. Lett. (1996) 77, 3865.
[13] Monkhorst H. J. and Pack J. D., Phys. Rev. B (1976) 13, 5188.
[14] Birch F. Phys. Rev. (1947) 71, 809.
[15]www.pwscf.org .
[16] Kubo Y., Ishida S. and Ishida J., J. Phys. F; Metal Phys. (1981) 11 2443-60.
[17] Ishida S., Asto H., Iwashima E., Kubo Y. and Ishida J., J. Phys. F; Metal Phys, (1981) 11, 1035-46.